RSC Advances

PAPER

View Article Online
View Journal | View Issue

Cite this: *RSC Adv.*, 2015, **5**, 49195

Support vector machine (SVM) classification model based rational design of novel tetronic acid derivatives as potent insecticidal and acaricidal agents†

Ting-Ting Yao,[a] Jing-Li Cheng,[a] Bing-Rong Xu,[a] Min-Zhe Zhang,[b] Yong-Zhou Hu,[b] Jin-Hao Zhao*[a] and Xiao-Wu Dong*[b]

Received 31st March 2015
Accepted 28th May 2015

DOI: 10.1039/c5ra05663b

www.rsc.org/advances

A novel support vector machine (SVM) classification model was established for distinguishing potent and weak/inactive insecticides. Classification model-based rational design of novel tetronic acid derivatives was then performed to choose the preferable site of spirotetramat for chemical modification. Afterwards, eleven C5′-oxime ether-derived spirotetramat analogues, which are indicated as "potent class", were synthesized and validated by biological assays, revealing that theoretical estimates are significantly consistent with experimental activities of these compounds. To be of interest, the most promising compound **91b** exhibited excellent insecticidal and acaricidal activities. Moreover, molecular docking was further implemented to propose the possible interaction mode of acetyl-CoA carboxylase (ACCase) and compounds **91b**, **91j**, and **91k**, providing some important and useful guidelines for further development.

1 Introduction

Tetronic acid derivatives, such as spirotetramat, spirodiclofen and spiromesifen (Fig. 1), have been developed as good insecticides in modern agriculture for the control of a broad spectrum of insects, such as aphids, whiteflies and psyllids, *via* the inhibition of acetyl-CoA carboxylase (ACCase).[1,2] Since the unique targeting characteristic, this kind of compounds are considered to be safer insecticides, rendering the scientists to perform extensively chemical optimization to explore the insecticide candidates with more potency and broader insecticidal spectrum.[3–5] So far, most of the efficient studies focused on C-4 and C-8 site of spirotetramat skeleton *via* application of traditional approaches, nevertheless, there are still some challenges needing to be addressed, such as low discovering efficacy and limited activities against mites,[6,7] promoting us to develop a novel series of tetronic acid derivatives with broader insecticidal spectrum, especially using more efficient method.

Due to the valuable quantitative realizations about the effect of functional groups for biological activities, some QSAR studies have been reported to assist the discovery of insecticides.[8–13] In this field, Moore *et al.* reported the pioneering QSAR work on the acaricidal activities using the Hansch approach.[8] Later, Sakashita *et al.* firstly demonstrated the application of quantum chemical parameters in the establishment of QSAR model.[9] In addition to 2D-QSAR, Yang *et al.*[10] and Okazawa *et al.*[11] described the development of 3D-QSAR models using CoMFA method to probe the 3D-requirement of pesticides for biological activities. To be of interest, it is also feasible for QSAR study of tetronic acid derivatives. Yang *et al.* revealed that 3D-QSAR models of CoMFA and CoMSIA with good predictive ability were constructed based on a series of phenylhydrazine substituted tetronic acid derivatives, providing a practical tool for guiding the design novel compounds.[12] We also found that the insecticidal activities of tetronic acid derivatives were remarkably correlated with quantum chemical and physicochemical parameters, including log *P*, LUMO, HOMO.[13] So far, all of the reported QSAR models of tetronic acids were performed with

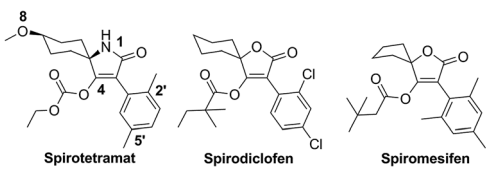

Fig. 1 The structure of representative tetronic acid derivatives.

[a]*Ministry of Agricultural Key Laboratory of Molecular Biology of Crop Pathogens and Insects, Institute of Pesticide and Environmental Toxicology, Zhejiang University, Hangzhou, 310029, People's Republic of China. E-mail: jinhaozhao@zju.edu.cn; Fax: +86-571-86971923; Tel: +86-571-86971923*

[b]*ZJU-ENS Joint Laboratory of Medicinal Chemistry, Zhejiang Province Key Laboratory of Anti-Cancer Drug Research, College of Pharmaceutical Sciences, Zhejiang University, Hangzhou, 310058, People's Republic China. E-mail: dongxw@zju.edu.cn; Fax: +86-571-88981051; Tel: +86-571-88981051*

† Electronic supplementary information (ESI) available: Fig. S1, S2 and Table S1, S2, S3. See DOI: 10.1039/c5ra05663b

regression approaches, thereby, they focused on only small sample sets of certain tetronic acids, owing to some limitations associated with regression methods: (1) the limited availability of consistent data for modelling; (2) the potential experimental error and interlaboratory variability present within the biological data.[14] In addition, the regression approaches mainly resolved the quantitative prediction of the model for active compounds, but ignoring the discrimination ability of the model for active and inactive compounds. In order to circumvent the problems of regression methods, more and more efforts have been placed into the development of relative flexible classification model, such as utilizing pattern recognition techniques. In this field, support vector machines (SVMs),[15,16] have been shown to perform well in the drug discovery process.[17,18] Indeed, we have demonstrated the establishment and application of SVM classification model in the identification of novel vasorelaxant agents.[19] To our knowledge, the classification model in rational design of tetronic acid derivatives is not disclosed so far. Therefore, the establishment of a SVM classification model for recognising tetronic acid derivatives as insecticide would still be of great interest.

Recently, we reported a series of spirotetramat derivatives with potent insecticidal and acaricidal activities using traditional approach,[3,13,20] however, the meticulous SARs of these compounds are not very clear, which requires much more effort to address these issues. Thus, we envisioned that the classification model of insecticides can be constructed, and that the rational design of novel insecticides can be accelerated by the assistance of classification model. In connection with our previous work on QSAR,[19,21–25] herein, we reported the first example of SVM classification model for distinguishing structurally diverse insecticides (n = 86) using a large set of molecular descriptors, and its successful application in rational design of novel spirotetramat derivatives (Scheme 1), affording a series of C5′-oxime ether-derived analogues **91a–91k** with good insecticidal activities against *Aphis fabae*. To our delight, the most potent compound **91b** also exhibited potent acaricidal activity against *Tetranychus cinnabarinus*. Furthermore, molecular docking was performed to explore the potential binding mode of ACCase with these spirotetramat derivatives.

2 Computational method

2.1 Dataset

A total of 86 structurally diverse compounds (Fig. 2) with different potency of insecticidal activities against *Aphis fabae* were taken from the recent literatures,[3,13,20,26] and randomly divided into training and test set, consisting of 66 molecules in training set and 20 molecules in test set. To reconcile the insecticidal activity (I%) against *Aphis fabae* at different concentrations (mg L^{-1}), biological data was converted to pseudo LD_{50} (pLD_{50}) according to the following steps: the mass-based concentration (mg L^{-1}) was transferred to mole-based one (C μmol L^{-1}); insecticidal activity (I%) was then converted to pLD_{50} ($pLD_{50} = -\log C + \log((100 - I)/I)$). All of the compounds were classified into potent set (with a $pLD_{50} \leq -3.00$) or weak/inactive set (with a $pLD_{50} > -3.00$) on the basis of pseudo LD_{50} (Table 1 and S1, ESI†). In general, the structures of compounds were sketched and optimized using Discovery Studio 2.5 software package (Accelrys, Inc. San Diego, CA).

2.2 Descriptors calculation and selection

The optimized molecules were transferred into Dragon software (developed by Milano Chemometrics and QSAR Group)[27] to calculate constitutional descriptors, topological descriptors, edge adjacency indices, burden eigenvalue descriptors, *etc.* After the calculation of the molecular descriptors, those that stayed constant for all molecules were eliminated, and pairs of variables with a correlation coefficient greater than 0.80 were classified as inter-correlated, and one of them in each correlated pair was deleted. Then, the resultant pool of descriptors with low correlation were further sent to a combined protocol of stepwise multiple linear regression (Stepwise-MLR) and feature selection (F-score),[28] with aim to select the most relevant descriptors for model building.

2.3 SVM modelling

The basic idea of SVM can be summarized as follows: (1) the input vectors are mapped to a higher dimensional feature space *via* kernel function; (2) linear division within the feature space

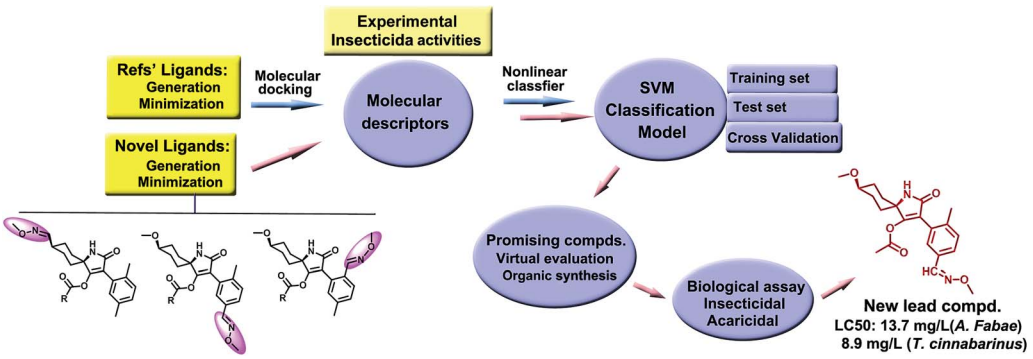

Scheme 1 The establishment of SVM classification model and its application in rational design of novel C5′-substituted spirotetramat derivatives as potent insecticidal and acaricidal agents.

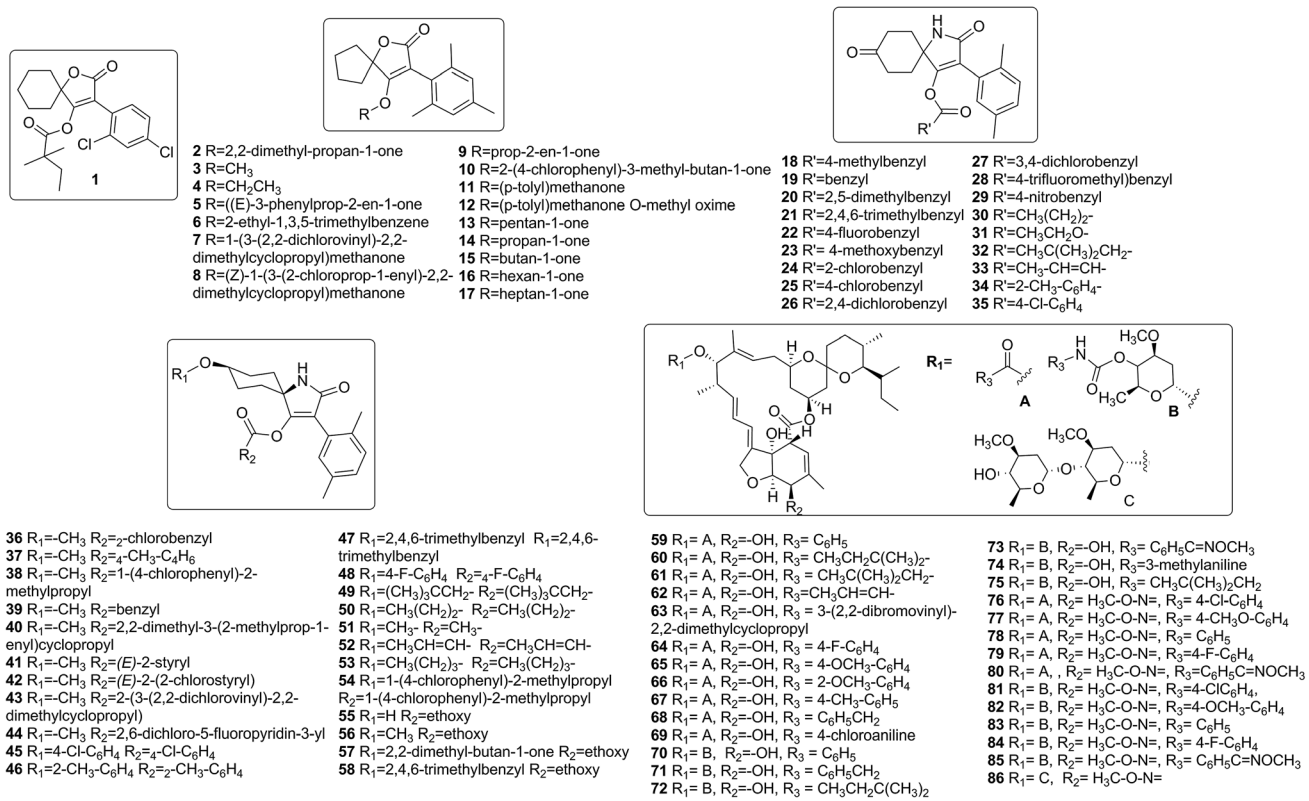

Fig. 2 The structures of insecticidal compounds **1–86** for SVM model development.

was optimized to construct a hyperplane with the largest margin separating classes of data. The decision function is as follow:

$$f(x) = \text{sign}\left(\sum_{i=1}^{l} y_i \alpha_i K(x, x_i) + b\right)$$

where sign is simply a sign function, which returns +1 for positive argument and −1 for a negative argument; y_i is input class label that takes a value of −1 or +1, x_i is a set of descriptors. $K(x, x_i) = \phi(x)\phi(x_i)$ is the kernel function, which is equal to the inner product of vectors x and x_i in the feature space $\phi(x)$ and $\phi(x_i)$.

2.4 Model validation

The quality of SVM model was measured by the values of sensitivity (eqn (1)), specificity (eqn (2)), accuracy (eqn (3)) and Matthews correlation coefficient (MCC) (eqn (4)). The value of MCC varies from −1 (complete disagreement between prediction of classes and observation) to +1 (perfect prediction), while 0 indicates a prediction no better than random.

$$\text{Sensitivity} = \frac{\text{TP}}{\text{TP} + \text{FN}} \quad (1)$$

$$\text{Specificity} = \frac{\text{TN}}{\text{TN} + \text{FP}} \quad (2)$$

$$\text{Accuracy} = \frac{\text{TP} + \text{TN}}{\text{TP} + \text{TN} + \text{FP} + \text{FN}} \quad (3)$$

$$\text{MCC} = \frac{\text{TP} \times \text{TN} - \text{FN} \times \text{FP}}{\sqrt{(\text{TP} + \text{FN})(\text{TP} + \text{FP})(\text{TN} + \text{FN})(\text{TN} + \text{FP})}} \quad (4)$$

where TP is the number of true positives, TN is the number of true negatives, FP is the number of false positives, and FN is the number of false negatives.

2.5 Sequence analysis and molecular docking

The amino acidic sequences of binding domain of ACCase enzyme from yeast and insects (*Panonychus citri* and *Tetranychus urticae*) were obtained from Swiss-Prot/TrEMBL database (http://expasy.org/). At first, we aligned them using alignment tool in Discovery studio 2.5 (Accelrys, Inc. San Diego, CA). Then, the molecular docking were performed by using LigandFit module embedded in Discovery Studio 2.5.[29] At first, the crystal structure of ACCase's CT domain of yeast was obtained from PDB bank (entry code: 3PGQ), and then was removed water molecules and charged by CHARMm force field. The active site was derived from the volume of co-crystal ligand. For generation of the ligands' conformations, variable numbers of Monte Carlo simulations were employed. All the calculations during the docking steps were performed under the PLP energy grid. A short rigid body minimization was then performed and 50 preferable poses were saved according to their dock score. Based on the dock score and visual inspection, the most possible pose was selected for the further analysis.

Table 1 Compounds in training set and test set for SVM classification model, and their corresponding experimental and theoretical classification

Compd	Exp. class[a] (pLD_{50} against *A. fabae*)	SVM-pred. class[c]	Compd	Exp. class[a] (pLD_{50} against *A. fabae*)	SVM-pred. class[c]
1	−1 (−2.57)	−1	**44**	1 (<−5.31)	1
2	−1 (−2.65)	−1	**45**	−1 (−1.82)	1
3	−1 (−1.99)	−1	**46**	−1 (−2.10)	−1
4[b]	−1 (−1.90)	−1	**47**	−1 (−2.47)	−1
5[b]	−1 (−2.82)	−1	**48**	−1 (−2.56)	−1
6	−1 (−1.94)	−1	**49**	−1 (−2.81)	−1
7	−1 (−2.26)	−1	**50**[b]	−1 (−2.74)	−1
8	−1 (−2.04)	−1	**51**	1 (−3.17)	1
9[b]	1 (−3.10)	1	**52**	−1 (−2.55)	−1
10	−1 (−1.69)	−1	**53**	−1 (−2.41)	−1
11	−1 (−2.81)	−1	**54**	−1 (−2.26)	−1
12	−1 (−2.94)	−1	**55**[b]	1 (−4.21)	1
13[b]	1 (−5.45)	1	**56**	1 (<−5.43)	1
14	1 (−3.23)	1	**57**	1 (−3.03)	−1
15	1 (−3.66)	1	**58**	−1 (−1.80)	−1
16	1 (−3.27)	1	**59**[b]	−1 (−2.97)	−1
17	1 (−3.51)	1	**60**	−1 (−1.58)	1
18[b]	−1 (−2.82)	1	**61**	−1 (−2.98)	−1
19	1 (−3.73)	1	**62**[b]	−1 (−2.93)	−1
20	−1 (−2.87)	−1	**63**	−1 (−2.79)	−1
21	−1 (−2.70)	−1	**64**	−1 (−2.57)	−1
22	1 (−3.54)	1	**65**	−1 (−2.92)	−1
23[b]	1 (−3.43)	1	**66**	−1 (−2.78)	−1
24	1 (−3.80)	1	**67**[b]	−1 (−2.56)	−1
25	1 (−3.30)	1	**68**	−1 (−2.68)	−1
26	1 (−3.10)	1	**69**	−1 (−2.75)	−1
27	1 (−3.89)	1	**70**[b]	1 (<−3.07)	−1
28	1 (−4.16)	1	**71**	1 (<−4.08)	1
29	1 (−3.42)	1	**72**	1 (<−3.48)	1
30[b]	1 (−4.23)	1	**73**	1 (<−3.05)	−1
31	1 (−3.51)	1	**74**	1 (<−4.06)	−1
32	−1 (−2.54)	−1	**75**[b]	−1 (−1.69)	1
33	1 (−3.13)	1	**76**	−1 (>1.58)	−1
34	−1 (−1.84)	−1	**77**[b]	−1 (−1.25)	−1
35	−1 (−2.62)	−1	**78**	−1 (−1.33)	−1
36[b]	−1 (−2.08)	1	**79**	−1 (>1.57)	−1
37	−1 (−2.96)	1	**80**[b]	−1 (−1.25)	−1
38	−1 (−2.33)	−1	**81**	−1 (−1.34)	−1
39	1 (−3.79)	1	**82**	−1 (−1.36)	−1
40[b]	1 (−3.17)	−1	**83**[b]	−1 (−1.16)	−1
41	1 (−3.68)	1	**84**	−1 (−1.46)	−1
42	1 (−3.09)	1	**85**	−1 (−1.61)	−1
43	−1 (−2.71)	−1	**86**	1 (<−3.36)	1

[a] Insecticidal activity scale against *A. fabae*: potent set with a $pLD_{50} \leq -3.00$ (1); weak/inactive set with a $pLD_{50} > -3.00$ (−1). [b] Test set. [c] The insecticidal activities scale was estimated by SVM classification model.

3 Results and discussion

3.1 Establishment of SVM classification model

After the correlation analysis, stepwise-MLR and feature selection, an optimal set of five molecular descriptors (PW3, Lop, R6m, EEig02r and BELm6, Table S2 and S3, ESI†), together with the squared log *P*, were finally selected for the classification modelling. Among them, squared log *P* is an equivalent measure of lipophilicity, which was found to be most correlated physicochemical parameters.[13] In addition to log *P*, the topological descriptors (PW3 and Lop) are the numerical quantifiers of the molecular topology; the GETAWAY descriptor (R6m) is a geometrical descriptor encoding information on the effective position of substituents and fragments in the molecular space; the Edge adjacency indices (EEig02r) encodes the connectivity between graph edges; the Burden eigenvalues (BELm6) can characterize the diagonal elements with atom weights. Indeed, all of these selected molecular descriptors provided the geometrical and topological features of the tested compounds, the features of which have been previously demonstrated to be optimal selections in other QSAR study.[30,31]

Because of the usage of radial basis function (RBF) as kernel function during SVM-classification modelling, the essential parameter RBF (γ) and capacity parameter (C) are needed to be

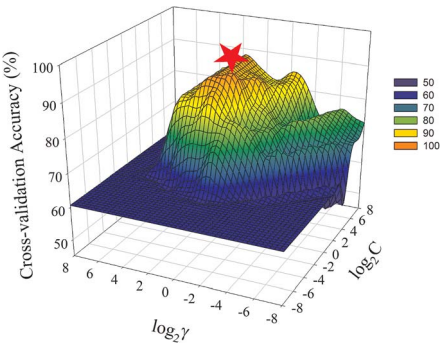

Fig. 3 The 3D plot of cross-validation accuracy for SVMs when choosing the optimal parameters γ and C.

optimized. Initially, intensive grid search method was applied in the process of leave-one-out (LOO) cross-validation to find the optimal parameters of γ and C, ranging from -8 to 8 of $\log_2 \gamma$ and $\log_2 C$ with increment steps of 1, respectively. To our delight, the best LOO cross-validation result (accuracy: 89.4%, Fig. 3) was obtained with an optimal value of 1 and 4 for γ and C, respectively. With the optimal parameters in hands, the SVM model was developed from the training set with a statistically significant performance (sensitivity: 92.3%, specificity: 97.5%, accuracy: 95.5%, MCC: 90.7%). For the twenty compounds in test set, the SVM model can correctly classify seventeen compounds (sensitivity: 85.7%, specificity: 84.6%, accuracy 85.0% and MCC 70.6%) (Fig. 4), the result of which demonstrated the accuracy and reliability of the established SVM model in categorizing structurally diverse compounds with potent or weak/inactive insecticidal activities.

3.2 Classification model-based rational design of novel insecticides

Considering that derivatives of spirotetramat shows good insecticidal activities but weak acaricidal activities, and the oxime ether moiety is a potent acaricidal pharmacophore,[32] we introduced oxime ether group to different site of spirotetramat skeleton, affording a set of analogues (Fig. S1, ESI†). Furthermore, the established SVM classification model was used to predict the potency of these newly designed compounds. To be

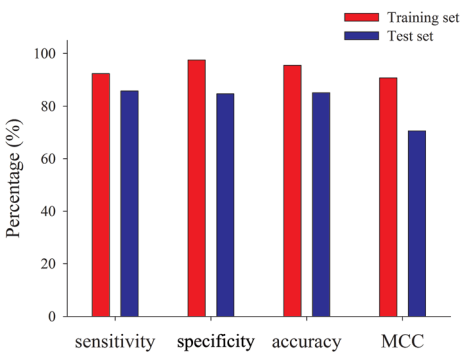

Fig. 4 Performance of the SVM classification model for the training and test sets.

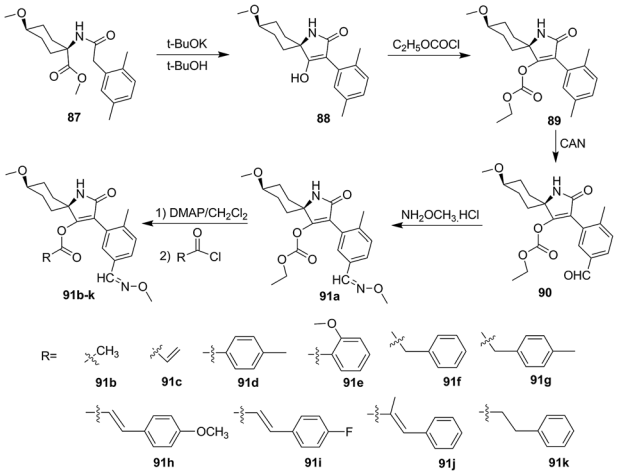

Scheme 2 Synthetic route for target compounds **91a–91k**.

of interest, all the compounds with oxime ether moiety onto C-5′ position of spirotetramat skeleton were estimated as potent insecticidal compounds, suggesting that C-5′ position is optimal for chemical modification. Accordingly, eleven compounds **91a–91k** (Scheme 2) bearing diverse side chains (*e.g.* methyl, vinyl, phenyl) on C-4 position of spirotetramat were selected for further study.

3.3 The synthesis of tetronic acid derivatives 91a–91k

The synthetic pathway of compounds **91a–91k** is outlined in Scheme 2. Initially, compound **88** was obtained through Dieckmann condensation of **87** in presence of potassium *tert*-butoxide. Successively esterification of **88** with ethyl chloroformate in room temperature afforded compound **89**, which was further oxidized by ceric ammonium nitrate (CAN) to afford **90**. The target compound **91a** was prepared by condensation of **90** with methoxyamine hydrochloride in anhydrous methanol. Finally, the synthesis of compounds **91b–91k** was achieved by acylation of **91a** with corresponding acyl chloride in presence of DMAP in CH_2Cl_2. The structures of compounds prepared were elucidated by ^{1}H NMR, ^{13}C NMR and HRMS.

3.4 Biological assay

The insecticidal activities of compound **91a–91k** were biologically evaluated against *Aphis fabae*, with commercial insecticide spirotetramat serving as a positive control. All of the biological assays were performed under a concentration of 100 mg L^{-1}. To our delight, the results indicated that most of the tested compounds showed potent insecticidal activities (Table 2), with more than 80% mortality rates against *Aphis fabae*, except for two misclassified compounds **91h** and **91j** with weak insecticidal activities, demonstrating the excellent predictive performance of SVM classification model. Moreover, three compounds **91b**, **91c** and **91k** with more than 90% mortality rates against *Aphis fabae* were further tested for their acaricidal activities against *Tetranychus cinnabarinus*, with aim to evaluate their insecticidal spectrum. To be of interest, compound **91b**

Table 2 Insecticidal and acaricidal activities of target compounds **91a–91k**

Entry	Exp. class[a] (pLD_{50})	Mortality against *A. fabae*[b] (LC_{50})[c]	Mortality against *T. cinnabarinus*[b] (LC_{50})[c]
91a	1(−3.10)	84%	—
91b	1(−3.92)	97% (13.7 mg L^{-1})	93% (8.9 mg L^{-1})
91c	1(−3.46)	92%	45%
91d	1(−3.09)	85%	—
91e	1(−3.19)	88%	—
91f	1(−3.24)	89%	—
91g	1(−3.04)	84%	—
91h	−1(−1.67)[d]	19%	—
91i	1(−3.03)	84%	—
91j	−1(−1.59)[d]	16%	—
91k	1(−3.33)	91%	13%
Spirotetramat		100% (5.1 mg L^{-1})[c]	75% (9.8 mg L^{-1})[c]

[a] The classification of compounds was provided by SVM model. [b] Mortality rate was determined at 100 mg L^{-1}. [c] Lethal concentration 50 value. [d] Misclassified compounds.

exhibited promising acaricidal activity with a LC_{50} value of 8.9 mg L^{-1}, revealing that the introduction of oxime ether moiety can exactly improve acaricidal activity of spirotetramat, and possibly extend the scope of application as miticide.

3.5 Molecular docking

In order to give a structural illustration for the experimental results above, molecular docking was performed to further explore the mechanism of newly developed spirotetramat derivatives. Due to the absence of crystal structure of carboxyltransferase domain of ACCase from insects, the structure from yeast (PDB ID code: 3PGQ) was employed as a surrogate, which shares a high sequence similarity (57.4% and 57.4%, respectively) with insects *Panonychus citri* and *Tetranychus urticae*, especially in the ligand binding site (92.2% and 92.2%, respectively) (Fig. S2, ESI†). The result of docking study showed that two hydrogen bonds and additional hydrophobic interaction served as important anchoring points for **91b**. As shown in Fig. 5A, the carbonyl oxygen on pyrrolone ring of **91b** is hydrogen-bonded to the amides of Ala1627 (2.68 Å) and Ile1735 (3.20 Å), and the oxygen of ethyl ester on the pyrrolone ring of **91b** formed additional H-bond with the amide of Gly1998 (2.17 Å), and the toluene group attached to pyrrolone ring of **91b** inserted into a hydrophobic pocket surrounded by Ile1735, Ala1672, Val2001, Val2002 and Phe1956 and Tyr1738. On the contrast, the binding mode of **91j**, which exhibited very weak insecticidal activities, was also docked into ACCase of yeast. To be of interest, no hydrogen bond were observed in proposed ACCase–**91j** complex (Fig. 5B), in which the orientation of carbonyl and the attached ethyl ester moiety on the pyrrolone ring was remarkably affected by the cinnamoyl group. Instead of toluene group attached to pyrrolone ring of **91j**, the cinnamoyl group inserted into the hydrophobic pocket surrounded by Ile1735, Ala1672, Val2001, Val2002 and Phe1956 and Tyr1738. Thus, the proposed interaction mode of **91j** is quite different from that of **91b**, which may cause their significantly different potency of insecticidal activities. Furthermore, molecular docking of **91k** was also performed to investigate the effect of more flexible moiety (phenylpropionyl group) on the binding

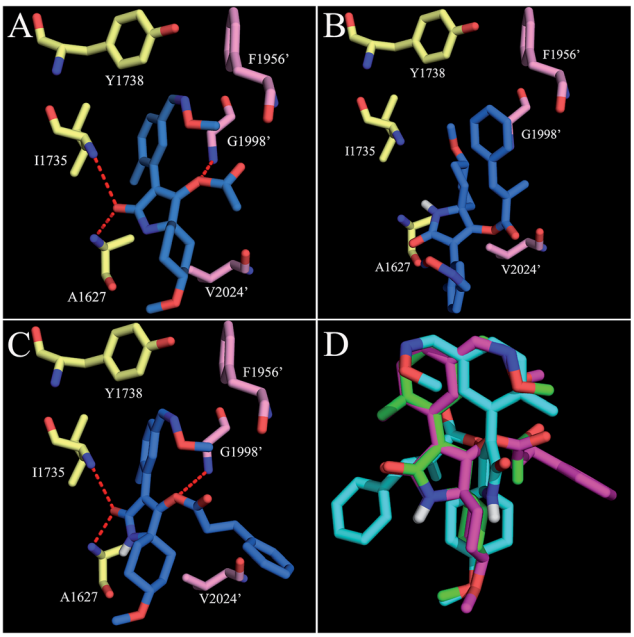

Fig. 5 Interaction mode of ACCase and **91b** (A), **91j** (B) and **91k** (C) proposed by molecular docking and their molecular overlay (D).

conformation of **91k**, revealing that the phenylpropionyl group can easily point to the surface of the binding pocket of ACCase, and the negative effect of the orientation of carbonyl on pyrrolone ring can be attenuated, thereby the essential hydrogen bond between the carbonyl oxygen on pyrrolone ring of **91k** and the amides of Ala1627 (2.55 Å) and Ile1735 (2.94 Å) can be observed (Fig. 5C). However, we could not exclude the other possibility caused by structural features for their different efficacy, considering that the ACCase used in present study is neither from *Aphis fabae* nor *Tetranychus cinnabarinus*.

4 Conclusion

Herein, we developed a SVM classification model with a statistically significant performance against training set and test set.

This model was further applied to rationally design novel tetronic acid derivatives as insecticide, resulting in the development of nine C-5′-oxime ether-derived tetronic acids with potent insecticidal activities against *Aphis fabae*. To be of interest, the most promising compound **91b** exhibited both of excellent insecticidal and acaricidal activities. The interaction modes between the potential target ACCase and compound **91b**, **91j** and **91k** were further explored to give a structural explanation for their different insecticidal activities. The good accordance of experimental activities and theoretical estimates renders this strategy a good complement in further development of novel insecticides.

5 Experimental section

5.1 Chemistry

^{1}H NMR and ^{13}C NMR spectra were recorded at 500 MHz using a Bruker AVANCE III spectrometer in $CDCl_3$, or DMSO-d_6 solution, with tetramethylsilane (TMS) serving as internal standard. Chemical shift values (δ) were reported in ppm. MALDI-TOF mass spectra were conducted on a Waters GCT Premier GC-TOFMA mass spectrometer. The melting points were determined on an X-4 binocular microscope melting point apparatus (Beijing Tech Instruments Co., Beijing, China) and are uncorrected. All of the reagents were distilled and dried by standard techniques prior to use when necessary.

5.1.1 Synthesis of *cis*-3-(2,5-dimethylphenyl)-4-hydroxy-8-methoxy-1-azaspiro[4.5]-dec-3-en-2-one (88). Potassium *tert*-butoxide (5.1 g, 45 mmol) was initially charged in 25 mL of dimethyl formamide and cooled on ice. A solution of **87** (30 g, 90 mmol) in 150 mL dimethyl formamide was added dropwise at 0 to 10 °C, and the mixture was stirred at 90 °C overnight. After removal of dimethyl formamide, residue was acidified with hydrochloric acid and partitioned between water and ethyl acetate. The organic layer was dried and distilled off. The mixture was purified by column chromatography on silica gel (dichloromethane/ethyl acetate = 1 : 1) to give **88**. Yield: 20.34 g (79% of theory); m.p. 225–227 °C; ^{1}H NMR (500 MHz, $CDCl_3$): δ 7.08 (d, J = 8 Hz, 1H, Ph–H), 6.99 (d, J = 8 Hz, 1H, Ph–H), 6.89 (s, 1H, Ph–H), 3.26 (s, 3H, –OCH_3), 3.10 (s, 1H, –NH), 1.41–1.98 (m, 8H, cyclohexane-H_8); TOF-MS: calcd for $C_{18}H_{23}NO_3$ 301.1678, found 301.1674.

5.1.2 Synthesis of *cis*-3-(2,5-dimethylphenyl)-8-methoxy-2-oxo-1-azaspiro[4.5]-dec-3-ene-4-ethylcarbonate (89). To a solution of **88** (7.89 g, 23.6 mmol) and triethylamine (5.29 g, 52.3 mmol) in dichloromethane (15 mL) was added dropwise a solution of ethyl chloroformate (4.26 g, 39.3 mmol) in anhydrous dichloromethane (80 mL). The reaction mixture was stirred at room temperature for 3.5 h until the reaction was completed, indicated by TLC. Afterward, the mixture obtained was extracted by dichloromethane, and the organic layer was concentrated and purified by column chromatography on silica gel with petroleum ether and ethyl acetate (v/v = 3 : 1) to give **89** as a white solid. Yield: 6.3 g (75% of theory); m.p. 141–142 °C; ^{1}H NMR (500 MHz, $CDCl_3$): δ 7.12 (d, J = 8.0 Hz, 1H, Ph–H), 7.05 (d, J = 8.0 Hz, 1H, Ph–H), 6.99 (s, 1H, Ph–H), 6.78 (s, 1H, –NH–), 4.04 (q, J = 7.0 Hz, 2H, –O–CH_2CH_3), 3.39 (s, 3H, –OCH_3), 3.27–3.22 (m, 1H, CH_3OCH–), 2.30 (s, 3H, Ar–CH_3), 2.27 (s, 3H, Ar–CH_3), 1.40–2.21 (m, 8H, cyclohexane-H_8), 1.12 (q, J = 7.0 Hz, 3H, –O–CH_2CH_3); TOF-MS: calcd for $C_{21}H_{27}NO_5$ 373.1889, found 373.1886.

5.1.3 Synthesis of *cis*-3-(5-formyl-2-methylphenyl)-8-methoxy-2-oxo-1-azaspiro[4.5]-dec-3-ene-4-ethylcarbonate (90). Compound **89** (18.7 g, 52 mmol), ceric ammonium nitrate (0.75 g, 5 mmol) and sodium bromate (0.75 g, 5 mmol) were added to acetonitrile (100 mL). The mixture was stirred for 12 h in the temperature ranging from 80 to 85 °C, and solvent was removed *in vacuo*. Water was added to the residue, and the aqueous solution was extracted with ethyl acetate. The separated organic layer was dried over anhydrous Na_2SO_4, filtered and concentrated. The mixture obtained was purified by column chromatography on silica gel with petroleum ether and ethyl acetate (v/v = 2 : 1) to give **90** as a white solid. Yield: 6.20 g (32% of theory); m.p. 197–198 °C; ^{1}H NMR (500 MHz, $CDCl_3$): δ 9.97 (s, 1H, –CHO), 7.80–7.78 (dd, J_1 = 2 Hz, J_2 = 8 Hz, 1H, Ar–H), 7.69 (d, J = 2 Hz, 1H, Ar–H), 7.43 (d, J = 8 Hz, 1H, Ar–H), 6.60 (s, 1H, –NH–), 4.05–4.01 (q, 2H, –CH_2–CH_3), 3.41 (s, 3H, –OCH_3), 3.29–3.25 (m, 1H, CH_3OCH–), 2.39 (s, 3H, Me–Ar), 2.26–1.39 (m, 8H, cyclohexane-H_8), 1.10 (t, 3H, –CH_2–CH_3); ^{13}C NMR (125 MHz, $CDCl_3$): δ 191.6, 169.3, 165.7, 149.8, 145.2, 134.4, 131.6, 131.2, 129.5, 129.4, 120.4, 65.9, 60.6, 55.9, 31.6, 28.33, 20.25, 13.74; TOF-MS: calcd for $C_{21}H_{25}NO_6$ 387.1682, found 387.1684.

5.1.4 Synthesis of *cis*-3-[5-(methoxyimino-methyl)-2-methylphenyl]-8-methoxy-2-oxo-1-azaspiro[4.5]dec-3-en-4-ethylcarbonate (91a). To a solution of **90** (2.0 g, 5.37 mmol) in 20 mL anhydrous methanol was added methoxyamine hydrochloride (756 mg, 6.20 mmol). The mixture was stirred at room temperature for 2 h and monitored by TLC. After removal of the solution, residue was poured into ice water (60 mL) to give crude product. The mixture was purified by column chromatography on silica gel with petroleum ether and ethyl acetate (v/v = 3 : 1) to give **91a** as a pale yellow oil. Yield: 1.97 g (88% of theory); ^{1}H NMR (500 MHz, $CDCl_3$): δ 8.02 (s, 1H, Ph–CH=N–), 7.52–7.50 (m, 1H, Ph–H), 7.35 (d, J = 1.55 Hz, 1H, Ph–H), 7.25 (d, J = 8.0 Hz, 1H, Ph–H), 6.58 (s, 1H, –NH–), 4.04–4.02 (m, 2H, CH_3–CH_2–O), 3.95 (s, 3H, =N–OCH_3), 3.40 (s, 3H, –OCH_3), 3.25–3.23 (m, 1H, CH_3OCH–), 2.30 (s, 3H, Me–Ar), 2.24–1.41 (m, 8H, cyclohexane-H_8), 1.13–1.11 (m, 3H, CH_3–CH_2–); TOF-MS: calcd for $C_{22}H_{28}N_2O_6$ 416.1947, found 416.1952.

5.1.5 Synthesis of *cis*-3-[5-(methoxyimino-methyl)-2-methylphenyl]-8-methoxy-2-oxo-1-azaspiro[4.5]dec-3-en-4-acetic acid ester (91b). Compound **91a** (100 mg, 0.24 mmol) was initially charged in 8 mL of anhydrous dichloromethane, and 4-dimethylamiopryidine (118 mg, 1.00 mmol) was added. The mixture was stirred at room temperature for 3 h. Afterward, acetyl chloride (29 mg, 0.36 mmol) in 2 mL anhydrous dichloromethane was added dropwise. Then, the mixture was stirred for another 1 h at room temperature until the reaction was completed, indicated by TLC. The reaction mixture was poured into ice water (60 mL) and extracted by dichloromethane (10 mL × 3). The organic layer was successively washed with 5% dilute hydrochloric acid (10 mL × 3), 5% aqueous sodium bicarbonate (10 mL × 3), saturated brine (10 mL × 3), and dried over anhydrous Na_2SO_4. After filtration, the solvent was distilled

off, and residue was purified by column chromatography on silica gel with petroleum ether and ethyl acetate (v/v = 4 : 1) to give **91b** as a yellow solid. Yield: 62.8 mg (68% of theory); m.p. 180–185 °C; ^{1}H NMR (500 MHz, $CDCl_3$): δ 8.02 (s, 1H, Ph–CH=N–), 7.50–7.48 (m, 1H, Ph–H), 7.31 (d, J = 1.55 Hz, 1H, Ph–H), 7.24 (d, J = 8.0 Hz, 1H, Ph–H), 6.60 (s, 1H, –NH–), 3.95 (s, 3H, =N–OCH_3), 3.40 (s, 3H, –OCH_3), 3.26–3.22 (m, 1H, CH_3OCH–), 2.30 (s, 3H, Me–Ar), 2.23–1.40 (m, 8H, cyclohexane-H_8), 2.08 (s, 3H, O=C–CH_3); TOF-MS: calcd for $C_{21}H_{26}N_2O_5$ 386.1842, found 386.1843.

5.1.6 The identical method of 91b was used to synthesize and purify compounds 91c–91k

Analytical data for ***91c***. Yield: 35%; ^{1}H NMR (500 MHz, $CDCl_3$): δ 8.01 (s, 1H, Ph–CH=N–), 7.48–7.46 (d, J = 8.0 Hz, 1H, Ph–H), 7.31 (s, 1H, Ph–H), 7.25–7.23 (d, J = 8.0 Hz, 1H, Ph–H), 6.71 (s, 1H, Ph–H), 3.96 (s, 3H, =N–OCH_3), 3.67–3.63 (m, 1H, CH_2=CH–), 3.39 (s, 3H, –OCH_3), 3.25–3.21 (m, 1H, CH_3OCH–), 2.84–2.80 (m, 2H, CH_2=CH–), 2.30 (s, 3H, Me–Ar), 2.23–1.40 (m, 8H, cyclohexane-H_8); TOF-MS: calcd for $C_{22}H_{26}N_2O_5$ 398.1842, found 398.1838.

Analytical data for ***91d***. Yield: 38%; m.p. 192–194 °C; ^{1}H NMR (500 MHz, $CDCl_3$): δ 8.01 (s, 1H, Ph–CH=N–), 7.87–7.85 (m, 2H, Ph–H), 7.43 (dd, $J_1 = J_2$ = 1.7 Hz, 1H, Ph–H), 7.37 (d, J = 1.6 Hz, 1H, Ph–H), 7.23 (d, J = 8.0 Hz, 2H, Ph–H), 7.18 (d, J = 8.0 Hz, 1H, Ph–H), 6.62 (s, 1H, –NH–), 3.93 (s, 3H, =N–OCH_3), 3.38 (s, 3H, –OCH_3), 3.23–3.21 (m, 1H, CH_3OCH–), 2.43 (s, 3H, Me–Ar), 2.33 (s, 3H, Me–Ar), 2.24–1.43 (m, 8H, cyclohexane-H_8); ^{13}C NMR (125 MHz, $CDCl_3$): δ 170.1, 165.6, 161.5, 148.45, 147.34, 145.4, 139.82, 139.37, 130.7, 130.6, 130.5, 130.3, 129.7, 129.6, 129.5, 129.4, 129.2, 128.6, 127.4, 126.6, 126.2, 124.9, 122.2, 119.9, 61.9, 60.9, 55.7, 31.9, 28.3, 21.8, 19.8; TOF-MS: calcd for $C_{27}H_{30}N_2O_5$ 462.2155, found 462.2157.

Analytical data for ***91e***. Yield: 42%; m.p. 199–201 °C; ^{1}H NMR (500 MHz, $CDCl_3$): δ 8.03 (s, 1H, Ph–CH=N–), 7.72–7.70 (m, 1H, Ph–H), 7.53–7.51 (m, 1H, Ph–H), 7.43 (dd, $J_1 = J_2$ = 1.65 Hz, 1H, Ph–H), 7.40 (d, J = 1.45 Hz, 1H, Ph–H), 7.22–7.20 (m, 1H, Ph–H), 6.98–6.96 (m, 2H, Ph–H), 6.54 (s, 1H, –NH–), 3.94 (s, 3H, =N–OCH_3), 3.87 (s, 3H, Ar–OCH_3), 3.39 (s, 3H, –OCH_3), 3.23–3.21 (m, 1H, CH_3OCH–), 2.35 (s, 3H, Me–Ar), 2.24–1.40 (m, 8H, cyclohexane-H_8); TOF-MS: calcd for $C_{27}H_{30}N_2O_6$ 478.2104, found 478.2102.

Analytical data for ***91f***. Yield: 39%; ^{1}H NMR (500 MHz, $CDCl_3$): δ 7.96 (s, 1H, Ph–CH=N–), 7.49–7.46 (m, 3H, Ph–H), 7.38–7.36 (m, 1H, Ph–H), 7.21–7.19 (m, 2H, Ph–H), 7.08–7.06 (m, 2H, Ph–H), 6.47 (s, 1H, –NH–), 3.97 (s, 3H, =N–OCH_3), 3.62 (s, 2H, Ph–CH_2–COO–), 3.38 (s, 3H, –OCH_3), 3.22–3.20 (m, 1H, CH_3OCH–), 2.33 (s, 3H, Me–Ar), 2.14–1.34 (m, 8H, cyclohexane-H_8); TOF-MS: calcd for $C_{27}H_{30}N_2O_5$ 462.2155, found 462.2166.

Analytical data for ***91g***. Yield: 30%; ^{1}H NMR (500 MHz, $CDCl_3$): δ 7.95 (s, 1H, Ph–CH=N–), 7.48–7.42 (m, 1H, Ph–H), 7.26–7.16 (m, 4H, Ph–H), 7.08–7.06 (m, 1H, Ph–H), 6.94–6.92 (m, 1H, Ph–H), 6.54 (s, 1H, –NH–), 3.96 (s, 3H, =N–OCH_3), 3.57 (s, 2H, Ph–CH_2–COO–), 3.38 (s, 3H, –OCH_3), 3.26–3.19 (m, 1H, CH_3OCH–), 2.34 (s, 3H, Me–Ar), 2.23 (s, 3H, Me–Ar), 2.18–1.38 (m, 8H, cyclohexane-H_8); TOF-MS: calcd for $C_{28}H_{32}N_2O_5$ 476.2311, found 476.2309.

Analytical data for ***91h***. Yield: 34%; m.p. 184–186 °C; ^{1}H NMR (500 MHz, $CDCl_3$): δ 7.99 (s, 1H, Ph–CH=N–), 7.62 (d, J = 15.9 Hz, 1H, Ar–CH=CH), 7.47–7.45 (m, 3H, Ph–H), 7.35 (d, J = 1.6 Hz, 1H, Ph–H), 7.22 (d, J = 7.95 Hz, 1H, Ph–H), 6.92–6.90 (m, 2H, Ph–H), 6.52 (s, 1H, –NH–), 6.24 (d, J = 15.75 Hz, 1H, Ar–CH=CH), 3.92 (s, 3H, =N–OCH_3), 3.86 (s, 3H, Ar–OCH_3), 3.40 (s, 3H, –OCH_3), 3.25–3.23 (m, 1H, CH_3OCH–), 2.33 (s, 3H, Me–Ar), 2.25–1.41 (m, 8H, cyclohexane-H_8); ^{13}C NMR (125 MHz, $CDCl_3$): δ 169.9, 165.6, 162.2, 161.9, 148.5, 148.2, 139.4, 130.8, 130.3, 129.6, 129.3, 128.5, 126.8, 126.3, 121.9, 114.5, 112.1, 61.8, 60.7, 55.9, 55.5, 31.9, 28.5, 21.5, 19.8. TOF-MS: calcd for $C_{29}H_{32}N_2O_6$ 504.2260, found 504.2265.

Analytical data for ***91i***. Yield: 29%; m.p. 159–161 °C; ^{1}H NMR (500 MHz, $CDCl_3$): δ 8.01 (s, 1H, Ph–CH=N–), 7.63 (d, J = 16 Hz, 1H, Ph–CH=CH–), 7.51–7.49 (m, 2H, Ph–H), 7.05–7.03 (m, 3H, Ph–H), 6.97 (d, J = 2.0 Hz, 2H, Ph–H), 6.54 (s, 1H, –NH–), 6.33 (d, J = 16 Hz, 2H, Ph–CH=CH–), 3.94 (s, 3H, =N–OCH_3), 3.39 (s, 3H, –OCH_3), 3.27–3.22 (m, 1H, CH_3OCH–), 2.35 (s, 3H, Me–Ar), 2.22–1.38 (m, 8H, cyclohexane-H_8); TOF-MS: calcd for $C_{28}H_{29}FN_2O_5$ 492.2061, found 492.2066.

Analytical data for ***91j***. Yield: 30%; ^{1}H NMR (500 MHz, $CDCl_3$): δ 8.00 (s, 1H, Ph–CH=N–), 7.50–7.48 (m, 1H, Ph–H), 7.46–7.37 (m, 7H, Ph–H), 7.24 (d, J = 8.0 Hz, 1H, Ph–H), 6.32 (s, 1H, –NH–), 3.92 (s, 3H, =N–OCH_3), 3.40 (s, 3H, –OCH_3), 3.28–3.24 (m, 1H, CH_3OCH–), 2.35 (s, 3H, Me–Ar), 2.27–1.41 (m, 8H, cyclohexane-H_8), 2.05–2.04 (m, 3H, O=C–CH_3); TOF-MS: calcd for $C_{29}H_{32}N_2O_5$ 488.2311, found 488.2316.

Analytical data for ***91k***. Yield: 36%; m.p. 173–174 °C; ^{1}H NMR (500 MHz, $CDCl_3$): δ 8.01 (s, 1H, Ph–CH=N–), 7.48–7.45 (m, 1H, Ph–H), 7.31–7.01 (m, 7H, Ph–H), 6.55 (s, 1H, –NH–), 3.95 (s, 3H, =N–OCH_3), 3.40 (s, 3H, –OCH_3), 3.12–3.08 (m, 1H, CH_3OCH–), 2.84–2.81 (m, 2H, Ph–CH_2–CH_2–), 2.71–2.68 (m, 2H, Ph–CH_2–CH_2–), 2.29 (s, 3H, Me–Ar), 2.14–1.27 (m, 8H, cyclohexane-H_8); TOF-MS: calcd for $C_{28}H_{32}N_2O_5$ 476.2311, found 476.2316.

5.2 Biological assay

All bioassays were performed on representative organisms reared in the laboratory. The bioassay was tested for triplicates at 25 ± 1 °C to take consideration of inter-batch variability. The variation of the measurement estimated over the total procedure is known to be approximately ±5%. Assessments were made on a dead/alive basis, and mortality rates were corrected using Abbott's formula. Evaluations were based on a percentage scale of 0–100, where 0 indicates no activity and 100 represents total kill. Spirotetramat was evaluated employing the same procedure as standard.

5.2.1 Inhibition activity against bean aphids (*Aphis fabae*). The insecticidal activities of target compounds and spirotetramat were evaluated according to the previously reported procedure.[33,34] Bean aphids were treated according to a slightly modified FAO dip test. Tender soybean shoots with fifty healthy third-instar nymphae were dipped into the diluted solutions of the compounds for 5 s, then superfluous fluid was removed, and the nymphae treated were placed in an conditioned room. Mortality was calculated 72 h after treatment. Each treatment

was performed in triplicates. These tests were implemented in parallel with a control treated by water only.

5.2.2 Inhibition activity against carmine spider mite (*Tetranychus cinnabarinus*). The larvicidal activities of target compounds and the contrast spirotetramat against *T. cinnabarinus* were measured on the basis of reported procedure.[35,36] Fifty third-instar mite larvae were dipped in the diluted solutions of tested chemicals for 5 s, the superfluous liquor was removed, and the larvae were kept in an conditioned room. Mortality rates were recorded 72 h after treatment. Each test was replicated three folds. Control groups treated with water only were tested under the same conditions.

Acknowledgements

This study was financially supported by Natural Science Foundation of Zhejiang Province, China (LY15C140002, LY13H300002) and Science and Technology Planning Project of Zhejiang Province (2014C37050).

Notes and references

1 E. Brück, A. Elbert, R. Fischer, S. Krueger, J. Kühnhold, A. M. Klueken, R. Nauen, J. F. Niebes, U. Reckmann, H. J. Schnorbach, R. Steffens and X. van Waetermeulen, *Crop Prot.*, 2009, **28**, 838–844.
2 R. Nauen, U. Reckmann, J. Thomzik and W. Thielert, *Bayer CropSci. J.*, 2008, **61**, 245–278.
3 J. L. Cheng, X. R. He, X. C. Wang, J. G. Zhang, J. H. Zhao and G. N. Zhu, *Pest Manage. Sci.*, 2013, **69**, 1121–1130.
4 Z. Liu, Q. Lei, Y. Li, L. Xiong, H. Song and Q. Wang, *J. Agric. Food Chem.*, 2011, **59**, 12543–12549.
5 S. Ke, Z. Zhang, Y. N. Zhang, L. Shi, R. Zhou, A. Jiang, Y. Liang and Z. Yang, *Res. Chem. Intermed.*, 2012, **38**, 1827–1837.
6 D. Marčić, P. Perić, S. Petronijević, M. Prijović and T. Drobnjaković, *Pestic. Fitomed.*, 2011, **26**, 185–195.
7 M. Basit, M. A. Saleem, S. Saeed and A. H. Sayyed, *Crop Prot.*, 2012, **40**, 16–21.
8 M. A. Dekeyser, D. M. Borth, R. C. Moore and A. Mishra, *J. Agric. Food Chem.*, 1991, **39**, 374–379.
9 T. Akagi and N. Sakashita, *Z. Naturforsch., C: J. Biosci.*, 1993, **48**, 345.
10 G. Yang, H. Liu and H. Yang, *Pestic. Sci.*, 1999, **55**, 1143–1150.
11 A. Okazawa, M. Akamatsu, A. Ohoka, H. Nishiwaki, W. Cho, Y. Nakagawa, K. Nishimura and T. Ueno, *Pestic. Sci.*, 1998, **54**, 134–144.
12 Y. Hu, J. Wang, A. Lu and C. Yang, *Bioorg. Med. Chem. Lett.*, 2014, **24**, 3772–3776.
13 J. H. Zhao, J. G. Zhang, B. R. Xu, Z. C. Wang, J. L. Cheng and G. N. Zhu, *J. Agric. Food Chem.*, 2012, **60**, 4779–4787.
14 M. T. D. Cronin, A. O. Aptula, J. C. Dearden, J. C. Duffy, T. I. Netzeva, H. Patel, P. H. Rowe, T. W. Schultz, A. P. Worth, K. Voutzoulidis and G. Schüürmann, *J. Chem. Inf. Comput. Sci.*, 2002, **42**, 869–878.
15 N. Cristianini and J. Shawe-Taylor, *An introduction to support vector machines and other kernel-based learning methods*, Cambridge university press, 2000.
16 B. Schölkopf and A. J. Smola, *Learning with kernels: support vector machines, regularization, optimization and beyond*, MIT press, 2002.
17 L. P. de Cerqueira, A. Golbraikh, S. Oloff, Y. Xiao and A. Tropsha, *J. Chem. Inf. Model.*, 2006, **46**, 1245–1254.
18 T. Kazutoshi, L. Bono, A. Dragan, K. Takio, K. Mikio, O. Natsuo and S. Takahiro, *Mol. Diversity*, 2010, **14**, 789–802.
19 X. W. Dong, Y. J. Liu, J. Y. Yan, C. Y. Jiang, J. Chen, T. Liu and Y. Z. Hu, *Bioorg. Med. Chem.*, 2008, **16**, 8151–8160.
20 J. H. Zhao, Z. C. Wang, M. H. Ji, J. L. Cheng, G. N. Zhu and C. M. Yu, *Pest Manage. Sci.*, 2012, **68**, 10–15.
21 X. W. Dong, C. Y. Jiang, H. Y. Hu, J.-Y. Yan, J. Chen and Y. Hu, *Eur. J. Med. Chem.*, 2009, **44**, 4090–4097.
22 X. W. Dong, Y. M. Zhao, X. Q. Huang, K. N. Lin, J. Z. Chen, E. Q. Wei, T. Liu and Y. Hu, *Eur. J. Med. Chem.*, 2013, **62**, 754–763.
23 W. H. Zhan, D. Q. Li, J. X. Che, L. R. Zhang, B. Yang, Y. Z. Hu, T. Liu and X. W. Dong, *Eur. J. Med. Chem.*, 2014, **75**, 11–20.
24 X. W. Dong, J. Y. Yan, D. Lu, P. Wu, J. D. Gao, T. Liu, B. Yang and Y. Z. Hu, *Chem. Biol. Drug Des.*, 2012, **79**, 691–702.
25 X. W. Dong, X. L. Zhou, H. Jing, J. Chen, T. Liu, B. Yang, Q. J. He and Y. Z. Hu, *Eur. J. Med. Chem.*, 2011, **46**, 5949–5958.
26 J. H. Zhao, X. J. Xu, M. H. Ji, J. L. Cheng and G. N. Zhu, *J. Agric. Food Chem.*, 2011, **59**, 4836–4852.
27 *DRAGON Software, Version 2.1*, 2002.
28 C. C. Chang and C. J. Lin, *ACM Trans. Intell. Syst. Technol.*, 2011, **2**, 1–27.
29 C. M. Venkatachalam, X. Jiang, T. Oldfield and M. Waldman, *J. Mol. Graphics Modell.*, 2003, **21**, 289–307.
30 A. M. Helguera, R. D. Combes, M. P. Gonzalez and M. N. D. S. Cordeiro, *Curr. Top. Med. Chem.*, 2008, **8**, 1628–1655.
31 E. Buyukbingol, A. Sisman, M. Akyildiz, F. Nur Alparslan and A. Adejare, *Bioorg. Med. Chem.*, 2007, **15**, 4265–4282.
32 Y. Li, C. Li, Y. Zheng, X. Wei, Q. Ma, P. Wei, Y. Liu, Y. Qin, N. Yang and Y. Sun, *J. Agric. Food Chem.*, 2014, **62**, 3064–3072.
33 Y. Zhao, Y. Li, X. Ou, P. Zhang, Z. Huang, F. Bi, R. Huang and Q. Wang, *J. Agric. Food Chem.*, 2008, **56**, 10176–10182.
34 Q. Zhao, Y. Li, L. Xiong and Q. Wang, *J. Agric. Food Chem.*, 2010, **58**, 4992–4998.
35 Y. P. Luo and G. F. Yang, *Bioorg. Med. Chem.*, 2007, **15**, 1716–1724.
36 H. Dai, Y. Q. Li, D. Du, X. Qin, X. Zhang, H. B. Yu and J. X. Fang, *J. Agric. Food Chem.*, 2008, **56**, 10805–10810.